Crystallization kinetics of a 2D system using molecular dynamics simulation

2010 J. Phys.: Condens. Matter 22 455106

(http://iopscience.iop.org/0953-8984/22/45/455106)

J. Phys.: Condens. Matter **22** (2010) 455106 (6pp) doi:10.1088/0953-8984/22/45/455106

Crystallization kinetics of a 2D system using molecular dynamics simulation

Luis Gustavo V Gonçalves and José Pedro Rino

Departamento de Física, Universidade Federal de São Carlos, 13.565-905, São Carlos, São Paulo, Brazil

E-mail: vieira@df.ufscar.br

Received 19 August 2010, in final form 26 September 2010
Published 28 October 2010
Online at stacks.iop.org/JPhysCM/22/455106

Abstract

We present a study about the crystallization behavior of a two-dimensional particle system via molecular dynamics simulation. The interaction potential used here is a modified version of the Lennard-Jones potential which has the square lattice as the stable crystal structure at zero-pressure. The growth rate and the thermodynamic melting point are determined using a system with a free surface in the x direction. We also performed simulations of a supercooled liquid system with periodic boundary conditions to estimate the nucleation rate, the critical nucleus size, and the time lag of nucleation. These properties are important tools for understanding the crystallization phenomenon in a variety of materials.

(Some figures in this article are in colour only in the electronic version)

1. Introduction

Crystallization is one of the most notable phenomena in physics. It can occur in several ways: via homogeneous nucleation, in which the new phase is formed out of random fluctuations from the parent phase, or via heterogeneous nucleation, when an external nucleant, such as dopants or the walls of a container, facilitates the birth of the new phase. When parent phases are involved, crystallization can occur from an undercooled liquid or from a glass above T_g (the vitreous transition temperature). Also, it can be a first-order transition, which is the case for three-dimensional materials, or mediated via a hexatic phase, as is described in the Kosterlitz–Thouless–Halperin–Nelson–Young theory for 2D melting and freezing [1].

In this paper we present a quantitative description of the two stages of crystallization, nucleation and growth, in a two-dimensional system using molecular dynamics (MD) simulations. With increasing interest in microstructures and colloidal systems for technological applications, the study of dynamics in 2D systems becomes of great importance. Also, 2D melting and freezing still constitute a major challenge for theorists. We hope that any efforts to elucidate basic aspects of 2D crystallization kinetics will be useful for scientists in several fields.

We set up a liquid-crystal coexistence state in order to calculate the melting point T_M for the system. An estimate of the growth rate was made using the same geometry as in the calculation of T_M (section 2.1). Nucleation was analyzed using constant-pressure bulk simulations. Different from our previous work, in which we studied pressure-induced phase transitions [2], the simulation box is not allowed to change shape. The simulation domain is allowed to change the volume isotropically, and the aspect ratio of the box remains constant. This restriction is necessary because in this work we are interested in the liquid phase, which cannot be simulated in the Parrinello–Rahman scheme [3, 4]. Alternatively, we could have used a constant-volume ensemble, as is the common choice for 2D simulations (see [5] and [6]). However, in order to mimic the behavior of a large, unbounded set of particles, a stress-free condition is the better choice when a system has drastic density changes during a simulation run. The hexatic phase cannot be observed because of the variable particle concentration [7] in the geometries used in our simulations.

The particles in our system interact through a modified version of the Lennard-Jones potential. This potential is a true representative of a large class of colloidal systems. Dolganov *et al* [8] reported polymorphic behavior in systems with droplets over a liquid substrate, in which both hexagonal and square symmetry were observed. Lieber *et al* [9] found, in oil-drop experiments, that a change in the concentration or in the frequency of bounce led to transitions between square and hexagonal symmetry. Also, Cluzeau *et al* [10] reported that impurities over liquid crystals could self-organize into square

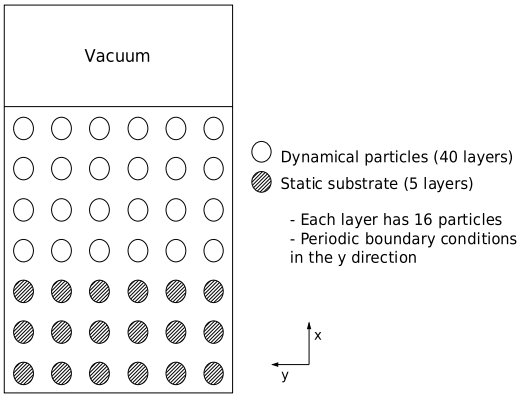

Figure 1. Schematic representation of the system over a substrate and with one free surface.

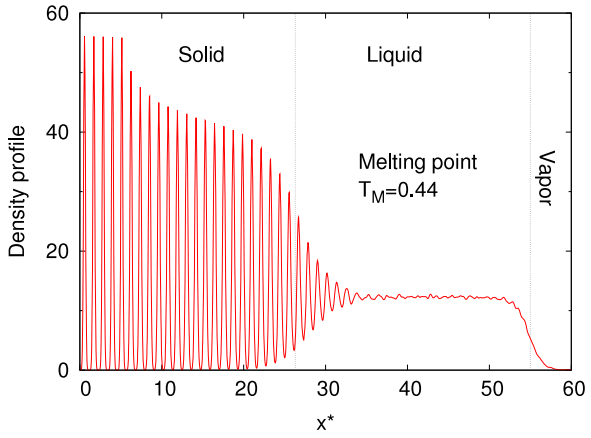

Figure 2. Density profile of the crystal–melt coexistence state.

and hexagonal lattices. Our system behaves in an analogous manner to such systems, i.e. by changing the pressure (or density) and the temperature.

2. Simulation procedure and results

Classical molecular dynamics (MD) simulation is the method employed in this work. It is based on integrating the coupled Newtonian equations of motion for a set of interacting particles. The interaction potential used in this work is the so-called modified Lennard-Jones potential [11]. The expression for this potential is

$$V_{\mathrm{MLJ}}(r) = -4\epsilon\left[\left(\frac{\sigma}{r}\right)^6 - \left(\frac{\sigma}{r}\right)^{12}\right] - G\mathrm{e}^{-\left(\frac{r-r_0}{\lambda}\right)^2}, \qquad (1)$$

where $G = 1.0\epsilon$, $\lambda = 0.2\sigma$ and $r_0 = 1.6\sigma$.

This potential is useful for mimicking self-organizing behavior in nanoparticle systems and colloidal matter [12, 2]. This choice of parameters gives rise to a double-well potential. The well that is the most distant from the origin lies exactly at the second-neighbor distance in a square lattice. In that way, particles in a stress-free condition organize themselves in a square symmetry. All physical properties reported here are in reduced units, i.e. energies are in units of ϵ and distances are in units of σ.

2.1. Melting point and growth rate

To calculate the melting point and to estimate the crystal growth rate, we set up a system described schematically in figure 1, known in the literature as slab geometry [13]. The particles are arranged initially in a square lattice (45 layers in the x direction, each layer has 16 particles, for a total of 720 particles) in which the first five layers remain static throughout the entire simulation. This static substrate has the purpose of eliminating surface effects in the bottom portion of the simulation box. To do so, the thickness of the substrate must be larger than the interaction cutoff. Thus, the dynamical layer adjacent to the substrate only 'sees' the perfect bulk structure. We added a vacuum region in the top portion to simulate surface effects. We applied periodic boundary conditions only in the y direction. We thus performed MD simulation in the microcanonical ensemble using a time step of $\Delta t = 0.005$. Preliminary simulations were run to estimate the lattice parameter of the system near the melting temperature at zero-pressure. The lattice parameter found was $a = 1.1$ which was used in the system to eliminate stress in the y direction. Heating was carried out by rescaling the velocity of particles. The structure of the slab was observed using the density profile defined as

$$\hat{\rho}_b(x) = \frac{1}{\sqrt{2\pi}d}\sum_{i=1}^{N} b_i \exp\left[\frac{-(x-x_i)^2}{2d^2}\right], \qquad (2)$$

where $b_i = 1$, d corresponds to 10% of the layer spacing and x_i is the x coordinate of the ith particle in a system of N particles.

Firstly, we obtained the thermodynamical melting point T_{M} using the phase-coexistence technique [13, 14]. Starting from the system in a square lattice over a static substrate and with one free surface, we heated the system until about half of the particles melted. We then stopped the heating process and let the system thermalize over a long microcanonical run (typically 80 000 time steps). The equilibrated solid–melt system must have a stable interface and its temperature, T_{M}, must be uniform along the direction normal to the interface. The melting point T_{M} was found to be 0.44(1) in reduced units. Figure 2 shows the density profile of the coexistence state.

The next step was to estimate the crystal growth rate [15] for the system. The particles in the first 15 layers over the substrate were frozen as we heated the remaining particles until melting of the dynamical portion. We then unfroze the previously static particles and let the system thermalize in a constant energy run.

In order to identify the crystal layer which is closest to the surface, we checked, in the density profile, the position of the last peak before the last valley with a density below 2.0. This is the maximum density value by which we could distinguish a crystal layer in configuration snapshots. The value of 2.0 for the particle density corresponds to, roughly, two-thirds of an entire layer formed. As an example, figure 3 shows the density profiles at two instants during crystallization. It was then possible to plot the number of crystal layers formed versus time. In figure 4 we present such a plot for three different initial

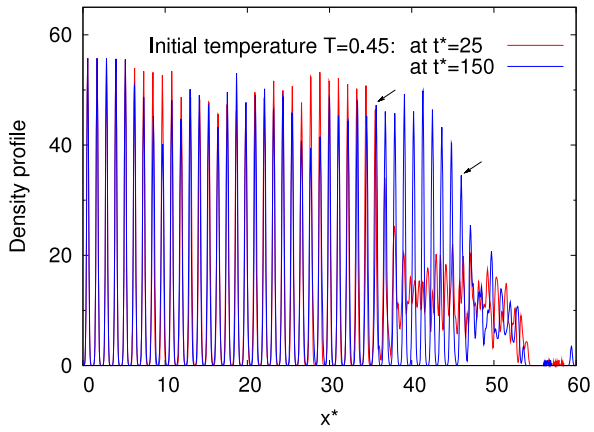

Figure 3. Density profiles of two instants during crystallization. The arrows indicate the 'crystallization front' advancing towards the surface.

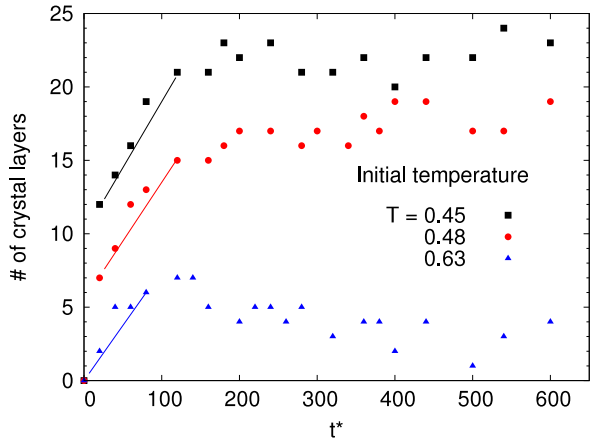

Figure 4. Number of crystal layers versus time for three initial temperatures of the dynamical portion. Rates were calculated using the slope of the lines plotted.

temperatures of the dynamical portion. The average growth rate in the linear regime was found to be 0.09 in reduced units (distance over time).

After the linear growth regime (figure 4), the crystallization front reaches an average plateau, which is about $4a$ thick. This can indicate a low value for the solid–liquid interfacial free energy, since thermal fluctuations are able to create or destroy a large amount of the crystal interface. The assumption is reinforced by noticing the extended solid–liquid interface in the coexistence averaged profile (figure 2).

2.2. *Nucleation from supercooled melt*

We performed constant-pressure MD simulations [16] without a variable box shape to study the homogeneous nucleation in a liquid–solid phase transition. The applied pressure was equal to zero in all simulations. We then set up a system with 3600 particles in a square lattice with periodic boundary conditions in the x and y directions.

The system was heated until a melt was obtained. The melt was subsequently cooled at several rates. The enthalpy

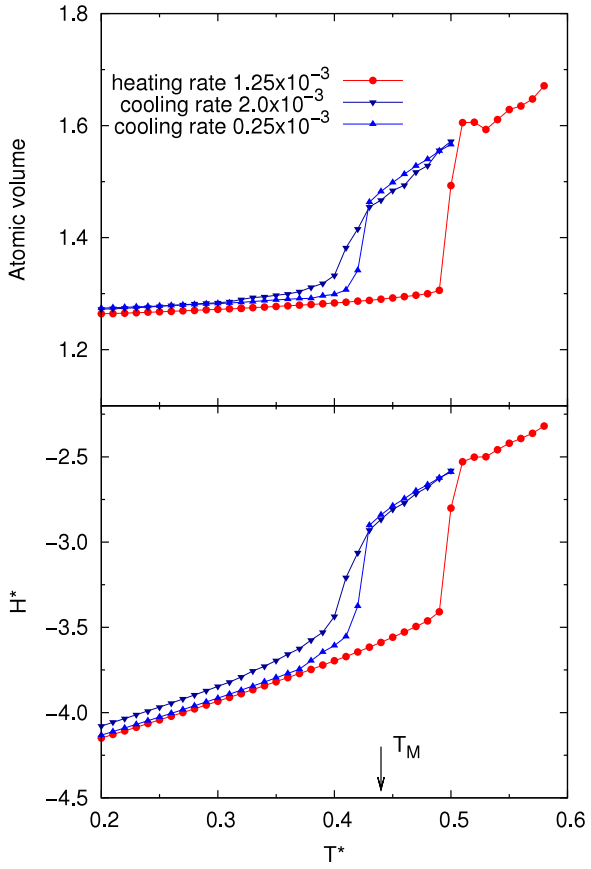

Figure 5. Atomic volume (top) and enthalpy (bottom) as a function of the temperature during heating of the perfect crystal and cooling of its melt using two distinct cooling rates. Rates are in units of energy over time.

and atomic volume as a function of the temperature in the heating process and at two different cooling rates is shown in figure 5. The enthalpy of fusion $\Delta H_f = 0.85$ was estimated using the height of the step during fusion. We were unable to obtain a glass from the melt. The glassy state of the system is highly metastable given that it would eventually crystallize independently of the cooling rate.

In order to determine in which phase the system is, we calculated the orientational space-correlation function $g_4(r)$ [6, 17], defined as

$$g_4(r) = \left\langle \frac{\sum_{i,j} \delta(r - \|\vec{r}_i - \vec{r}_j\|)\psi_4{}^*(\vec{r}_i)\psi_4(\vec{r}_j)}{\sum_{i,j} \delta(r - \|\vec{r}_i - \vec{r}_j\|)} \right\rangle, \quad (3)$$

where $\psi_4(\vec{r}) \equiv N_c^{-1} \sum_\alpha \exp[4i\theta_\alpha(\vec{r})]$ and $\theta_\alpha(\vec{r})$ is the angle of a given particle with the αth nearest neighbor relative to an arbitrary reference axis. The summation is over N_c neighbors. Particles are considered nearest neighbors if they are within a cutoff distance of 1.37 (see also the appendix).

Figure 6 shows the log–log plot of $g_4(r)$ for four temperatures during heating and at $T = 0.40$ after crystallization. The plot indicates the absence of the hexatic phase during melting since correlation functions are either of long-range (monocrystal) or short-range (liquid and polycrystal) orientational order.

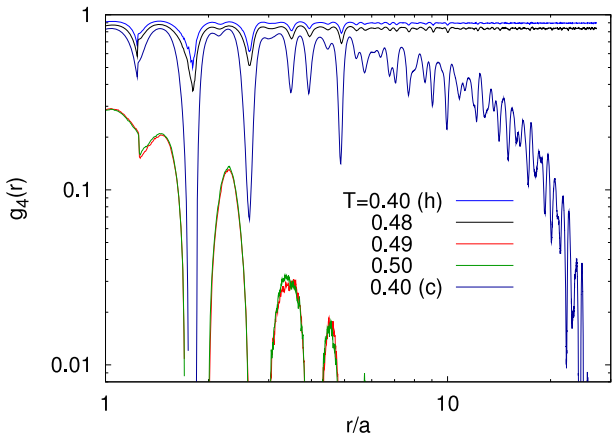

Figure 6. Orientational space-correlation function $g_4(r)$ in a log–log plot as a function of the temperature. At $T = 0.40$, correlations during heating (h) and cooling (c) are shown. Crystallization from supercooled liquid leads to the formation of a polycrystal, resulting in a loss of long-range orientational order.

Next, we calculated dynamical properties during transient states from a metastable undercooled liquid [18]. The temperature was held fixed and we monitored the non-Gaussian parameter α_2 given by [19]

$$\alpha_2(t) = \frac{\langle r^4(t)\rangle}{2\langle r^2(t)\rangle^2} - 1, \tag{4}$$

where $\langle r^2(t)\rangle$ and $\langle r^4(t)\rangle$ are, respectively, the mean-square and mean-quartic displacements.

Additionally, we quantified the number of solid-like particles and the largest cluster being formed during thermalization. We identify a solid-like particle using the ten Wolde [20] criterion and adapted it to our two-dimensional geometry. A detailed description of the criterion is found in the appendix. Results of the evolution of crystallization are shown in figure 7 at a temperature $T = 0.40$ (9.1% of undercooling).

In figure 7, the total number of solid-like particles starts to grow abruptly, marking the onset of nucleation [18]. From that instant, the largest nucleus observed reaches a size that never diminishes with time. This is an indication that nuclei above that critical size are always growing. Thus, we can estimate the critical nucleus size as the average of the largest nucleus before the onset of nucleation. The non-Gaussian parameter prior to the onset shows a large peak, which is an indication of dynamical heterogeneities present in the supercooled liquid [21].

Having found an estimate of the critical nucleus size, we can evaluate the nucleation rate of crystallization. We monitored the time evolution of the number of supercritical clusters, i.e. clusters larger than the critical size, and analyzed the linear behavior of nucleation. Since nucleation is a rare event, three conditions must be satisfied in order to evaluate the nucleation rate using 'brute force' MD: (1) a sufficient degree of undercooling; (2) a large system compared with the critical nucleus size; and (3) a sufficient number of samples to obtain good statistics. To fulfill the third condition, we prepared ten different samples of the system in the same

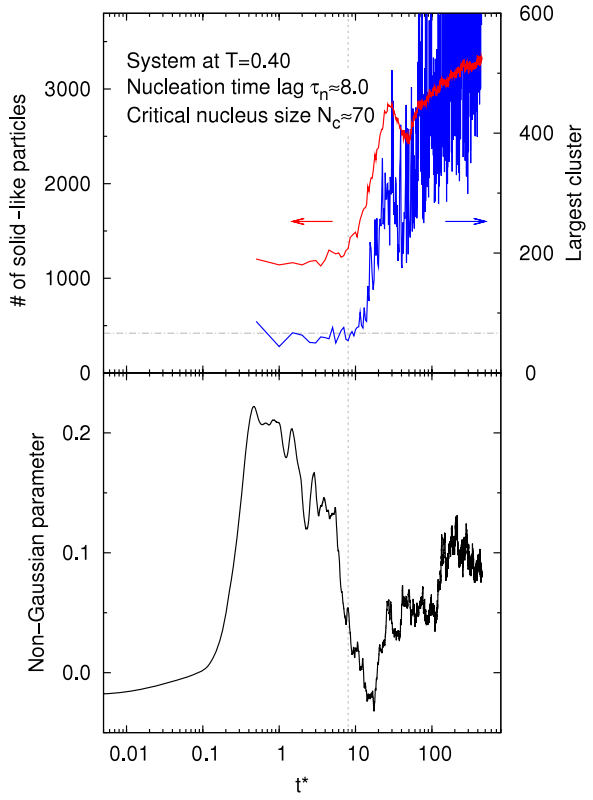

Figure 7. Evolution of the number of solid-like particles and the largest cluster (top) and the non-Gaussian parameter (bottom). The short-dashed vertical line indicates the onset of nucleation, from which we can estimate the critical nucleus size (dot-dashed horizontal line).

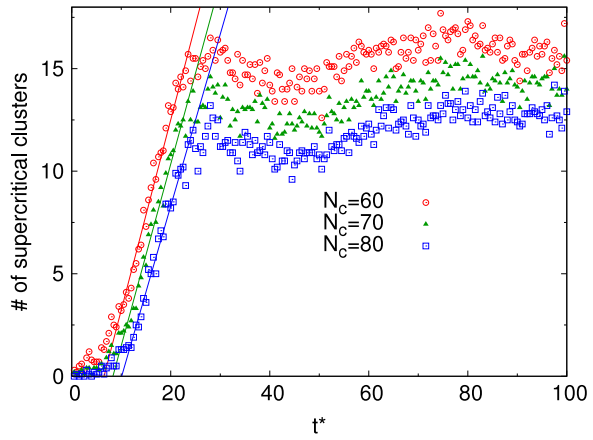

Figure 8. Number of clusters above a threshold size N_c averaged from ten samples under the same conditions. Lines correspond to linear fit in the nucleation regime. The nucleation rates found for $N_c = 60$, 70 and 80 were, respectively, 1.8×10^{-4}, 1.7×10^{-4} and 1.6×10^{-4} in reduced units.

thermodynamical conditions. Data from those simulations were averaged and results are shown in figure 8. Based on the Yasuoka–Matsumoto method [22] for evaluating condensation rates, we computed the nucleation rate J using three values of critical cluster size N_c. Similar slopes for the three N_cs indicate that the intermediate value of 70 makes a good estimate for the critical cluster size.

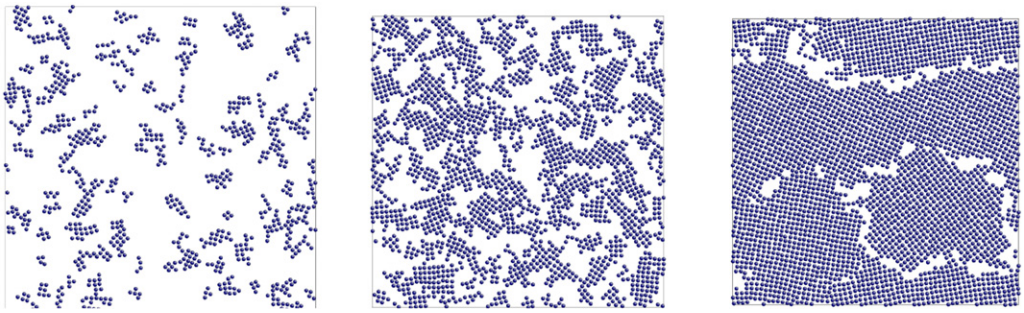

Figure 9. Snapshots of the system during crystallization at $T = 0.40$. Only solid-like particles are shown. Configuration at the onset of nucleation in (a), at $t^* = 24$ in (b) and the equilibrated configuration at $t^* = 450$ in (c).

Table 1. Critical nucleus size N_c, nucleation time lag τ_n, and nucleation rate J for two quenching temperatures.

T	Undercool.%	N_c	τ_n	J ($\times 10^{-4}$)
0.4	9.1	70	8.0	1.7
0.3	31.8	70	6.0	2.4

The same procedure was applied for a quenching temperature of 0.30. Results for critical nucleus size, nucleation time lag and nucleation rate are listed in table 1 for both temperatures. At a deeper undercooling, we found that the critical nucleus size remained unchanged. However, the system started to crystallize sooner and at a faster rate. Those results are in agreement with recent works [23, 24] in three-dimensional systems.

Figure 9 shows configuration snapshots for three instants during crystallization at $T = 0.40$. For a more efficient analysis, only solid-like particles are visible. The snapshots were generated using Li's ATOMEYE configuration viewer [25]. Different from our previous work [2], the system crystallized into a polycrystal rather than a monocrystal. This is a strong indication that system size effects were present in our previous simulations. Besides, the growth rate found in section 2.1 (0.09) tells us that roughly one crystal layer is created per ten time units. In that timespan, on the other hand, about ten supercritical clusters are spontaneously created at $T = 0.40$ (a critical cluster is 8–10 layers wide). Thus, nucleation is the dominant process of crystallization. This situation favors the formation of polycrystals, since it takes longer for domains to grow in a preferred direction. Figure 9(c) shows that this is in fact the case, where we can see at least four well-defined crystalline domains in the equilibrated configuration. Another remarkable feature of the nucleation process is the coalescence of small crystallites into larger clusters. This ripening-like behavior is in excellent qualitative agreement with recent observations made by Dillmann *et al* [26] in experiments with a two-dimensional colloidal system.

3. Conclusions

This work had the goal of describing and elucidating important aspects of crystallization using a low-packed two-dimensional system as a model. First, we estimated the ability of a crystal to grow from a seed in one direction (epitaxial growth). Such a procedure often yields an underestimated growth rate. Nevertheless, it gives us a good hint of the timescale in the growth regime. After we had discovered that the system melts via a first-order transition, we determined the melting point using the phase-coexistence method.

The main topic of the paper, crystallization kinetics, was studied using 'brute force' MD simulation under a condition of zero pressure. We first elaborated unambiguous criteria to spot crystalline clusters in the parent liquid phase. We were then able to monitor the formation of clusters in time. We concluded that: (1) the quenching temperature did not affect the critical nucleus size; (2) at a higher degree of supercooling, the system crystallized sooner and at a faster rate; and (3) the system solidified into a polycrystal via a ripening-like process. The first two conclusions show remarkable similarities with previous simulations of three-dimensional systems at deep supercooling conditions. The third conclusion is a direct consequence of the interplay between the growth rate, which was calculated using surface geometry, and the nucleation rate obtained in bulk simulations.

Acknowledgments

The authors would like to thank the Coordenação de Aperfeiçoamento de Pessoal de Nível Superior (CAPES), the Conselho Nacional de Desenvolvimento Científico e Tecnológico (CNPq), and the Fundação de Amparo à Pesquisa do Estado de São Paulo (FAPESP) for financial support.

Appendix. Parameters for the ten Wolde criterion

For each particle i, we calculated the complex vector $q_{4,m}$ defined as

$$q_{4,m}(i) = \frac{\bar{q}_{4,m}(i)}{[\bar{q}_{4,m}(i) \cdot \bar{q}^*_{4,m}(i)]^{1/2}} \tag{A.1}$$

and

$$\bar{q}_{4,m}(i) = \frac{1}{N_b(i)} \sum_j \Upsilon_{4,m}(\theta_{ij}, \phi_{ij}) \tag{A.2}$$

where the sum is taken over all j neighbors of i and $N_b(i)$ is the number of neighbors of particle i. $\Upsilon_{4,m}(\theta_{ij}, \phi_{ij})$ are spherical harmonic functions calculated using the angles θ_{ij}

and ϕ_{ij} formed by the distance vector $\vec{r}_i - \vec{r}_j$ and the x-axis as a frame of reference. In two dimensions, we set $\cos(\theta_{ij}) = 0$ since the particles are restricted to the xy-plane. Particles within a cutoff distance of 1.37 (i.e. the first minimum of the pair distribution function) were considered neighbors.

After we calculated $q_{4,m}(i)$, we computed the scalar product $q_{4,m}(i) \cdot q^*_{4,m}(j)$ for every particle i with each of its neighboring particles j. A particle was considered to be solid-like when at least three of the scalar products were greater than 0.5. Two neighboring solid-like particles were considered to belong to the same cluster. We only considered crystalline clusters (or crystallites) which had no fewer than four particles.

References

[1] Keim P, Maret G and von Grünberg H H 2007 Frank's constant in the hexatic phase *Phys. Rev.* E **75** 031402

[2] Damasceno P F, Gonçalves L G V, Rino J P and de Oliveira R de C M T 2009 Pressure-induced structural phase transitions in a two-dimensional system *Phys. Rev.* B **79** 104109

[3] Parrinello M and Rahman A 1980 Crystal-structure and pair potentials—a molecular-dynamics study *Phys. Rev. Lett.* **45** 1196

[4] Filion L, Marechal M, van Oorschot B, Pelt D, Smallenburg F and Marjolein Dijkstra M 2009 Efficient method for predicting crystal structures at finite temperature: variable box shape simulations *Phys. Rev. Lett.* **103** 188302

[5] Naidoo K J and Schnitker J 1994 Melting of two-dimensional colloidal crystals: a simulation study of the Yukawa system *J. Chem. Phys.* **100** 3114

[6] Muto S and Aoki H 2000 Molecular dynamics study of a classical two-dimensional electron system: positional and orientational orders *Physica* E **6** 116

[7] Gasser U 2009 Crystallization in three- and two-dimensional colloidal suspensions *J. Phys.: Condens. Matter* **21** 203101

[8] Dolganov P V, Demikhov E I, Dolganov V K, Bolotin B M and Krohn K 2003 *Eur. Phys. J.* E **12** 593

[9] Lieber S I, Hendershott M C, Pattanaporkratana A and Maclennan J E 2007 *Phys. Rev.* E **75** 056308

[10] Cluzeau P, Joly G, Nguyen H T and Dolganov V K 2002 *JETP Lett.* **75** 482

[11] Lee K Y and Ray J R 1989 Mechanism of pressure-induced martensitic phase-transformations—a molecular-dynamics study *Phys. Rev.* B **39** 565–74

[12] Engel M and Trebin H R 2007 Self-assembly of monatomic complex crystals and quasicrystals with a double-well interaction potential *Phys. Rev. Lett.* **98** 225505

[13] Chen E T, Barnett R N and Landman U 1989 Crystal–melt and melt–vapor interfaces of nickel *Phys. Rev.* B **40** 924

[14] Häkkinen H and Manninen M 1992 Computer-simulation of disordering and premelting of low-index faces of copper *Phys. Rev.* B **46** 1725–42

[15] Okada I, Abe Y, Nakata K, Baluja S, Aizawa M, Uchida H and Itatani K 2003 MD simulation of crystal growth from $CaCl_2$ melt *J. Mol. Liq.* **103** 371–85

[16] Andersen H C 1980 MD simulations at constant pressure and/or temperature *J. Chem. Phys.* **72** 2384

[17] Branício P S, Rino J P and Studart N 2001 Melting and orientational order of the screened Wigner crystal on helium films *Phys. Rev.* B **64** 193413

[18] Pang H, Jin Z H and Lu K 2003 Relaxation, nucleation, and glass transition in supercooled liquid Cu *Phys. Rev.* B **67** 094113

[19] Matsui G and Kojima S 2002 Bifurcation of translational and rotational non-Gaussian behaviors in two-dimensional liquid *Phys. Lett.* A **293** 156–60

[20] ten Wolde P R, Ruiz-Montero M J and Frenkel D 1996 Numerical calculation of the rate of crystal nucleation in a Lennard-Jones system at moderate undercooling *J. Chem. Phys.* **104** 9932–47

[21] Kob W, Donati C, Plimpton S J, Poole P H and Glotzer S C 1997 Dynamical heterogeneities in a supercooled Lennard-Jones liquid *Phys. Rev. Lett.* **79** 2827–30

[22] Yasuoka K and Matsumoto M 1998 Molecular dynamics of homogeneous nucleation in the vapor phase. I: Lennard-Jones fluid *J. Chem. Phys.* **109** 8451–62

[23] Koishi T, Yasuoka K and Ebisuzaki T 2003 Large scale molecular dynamics simulation of nucleation in supercooled NaCl *J. Chem. Phys.* **119** 11298–305

[24] Valeriani C, Sanz E and Frenkel D 2005 Rate of homogeneous crystal nucleation in molten NaCl *J. Chem. Phys.* **122** 194501

[25] Li J 2003 Atomeye: an efficient atomistic configuration viewer *Model. Simul. Mater. Sci. Eng.* **11** 173

[26] Dillmann P, Maret G and Keim P 2008 *J. Phys.: Condens. Matter* **20** 404216